Kinetics of Particle Growth in a Fluidized Calciner

B. S. LEE and JU CHIN CHU
Polytechnic Institute of Brooklyn, Brooklyn, New York
A. A. JONKE and STEPHEN LAWROSKI
Argonne National Laboratory, Argonne, Illinois

This study of the factors underlying the mechanisms of particle growth in a fluidized calciner was conducted in a 3-in. diameter column. In such a calciner radioactive waste liquor from nuclear fuel reprocessing can be converted to a granular solid for disposal. To simulate the actual waste, aluminum oxide as bed material and aqueous aluminum nitrate solution as feed were used. Particle growth was traced through the addition of radioactive seeds. The effects on the growth rate of operating variables and physical properties of the feed were investigated. Statistical analysis of the data substantiated the proposed growth mechanism, and the resulting growth coefficient was correlated with the variables studied.

Fluidized calcination is a process that incorporates the features of spray drying and fluidization. A feed solution containing dissolved solids is atomized by a spray nozzle and injected into a heated bed of fluidized particles in which the feed is dried and calcined and from which product is continuously withdrawn. This process offers in addition to continuous operation, good heat transfer characteristics, and uniform bed temperature the ease of remote control and the absence of moving parts that require seals or packings. The last two features render this process particularly attractive to the nuclear energy field, where the radioactivity must be contained.

In the nuclear energy field one area of application for fluidized calcination is in the conversion of liquid radioactive wastes from the reprocessing of nuclear fuels to solid form (*7, 10*). At present no established method has been found for ultimate disposal, and the waste liquor is stored in large underground tanks (*18*). The type of waste under study here is an aluminum nitrate solution containing fission products, the volume of which now stored is on the order of ten million gallons (*14*). Of the various processes proposed for reducing wastes to solids, fluidized calcination is among the most promising, having achieved a volume reduction of six or eight to one (*7*). A 2-ft. square calciner has been constructed at the Idaho Chemical Processing Plant (ICPP) and is now operating (*6*).

The stability of operation of a fluidized calciner depends on the control of the size of the particles in the unit. The two chief mechanisms contributing to changes in particle size are normal growth due to the continuous addition of feed and attrition due to both interparticle collisions and particle-atomizing gas action. To investigate these mechanisms the system chosen was an aqueous aluminum nitrate solution similar to the waste liquor but without radioactivity.

From work done at the Argonne National Laboratory (ANL) on fluidbed calcination of uranyl nitrate to uranium oxide (*3, 7, 16*) it was found that the rate of feeding, the solids content in the feed, the nozzle atomizing gas flow rate, the fluidizing gas flow rate, and the temperature of the fluidized bed were factors that affected particle growth. The effects of these variables on particle growth and some physical properties of the feed solution were studied in this project.

The control of particle size in fluid coking process has been described (*5*), including equations for steady state particle distribution. A number of papers (*4, 11, 18*) dealt with particle size variation in spray drops with only qualitative conclusions.

ANALYSIS OF PARTICLE GROWTH

With regard to the normal growth of the particle, consider a particle of diameter D. This particle grows only while passing through the zone formed by the spray droplets. When one assumes that the mass rate of growth in this zone is proportional to the surface of the particle, then

$$\frac{dm}{d\theta_s} = kD^2 \qquad (1)$$

However as θ_s is not a readily measurable quantity, it is converted to θ_F through the following:

$$\frac{d\theta_s}{d\theta_F} = k_1 \frac{V_s}{V_T}$$

where k_1 accounts for deviations from uniformity in bed density in the spray zone due to the injection of feed and the atomizing gas. Thus when one defines a normal growth coefficient $K = k\,k_1 \frac{V_s}{V_T}$, Equation (1) becomes

$$\frac{dm}{d\theta_F} = KD^2 \qquad (2)$$

Analyzing the factors affecting K, consider V_s as

$$V_s = k_2\left(\frac{\rho_{bs} - \rho_{bF}}{\rho_{bs}}\right)V_s'$$

where k_2 accounts for the distortion of the spray zone by the fluidized solids.

Moreover as $\rho_{bs} = \frac{W}{L_s A_c}$ and $\rho_{bF} = \frac{W}{L_F A_c}$, upon substitution

$$K = k\,k_1\,k_2 \frac{V_s'}{L_F A_c}\left(1 - \frac{L_s}{L_F}\right) \qquad (3)$$

B. S. Lee is with Arthur D. Little, Inc., Cambridge, Massachusetts.

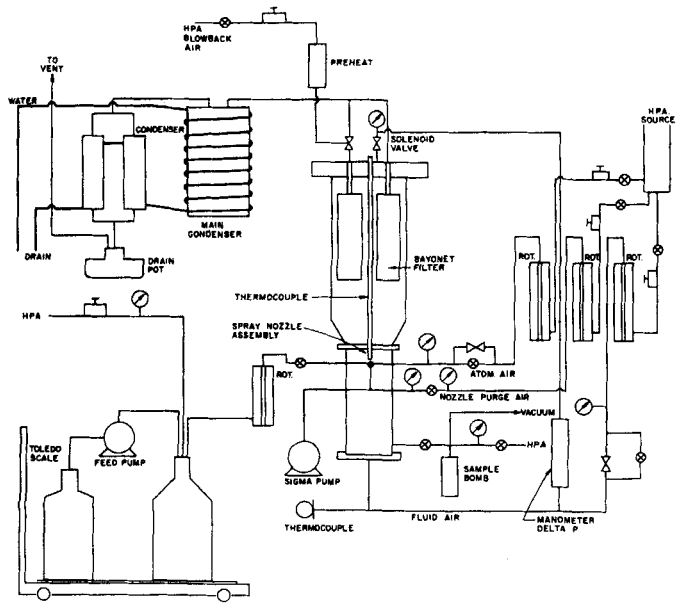

Fig. 1. Schematic layout and auxiliary equipment for the 3-in. fluidized calciner.

Now correlating L_F with ϵ through

$$\epsilon = 1 - \frac{L_o}{L_F}$$

where $L_o = \dfrac{W}{\rho_s A_c}$, and substituting in Equation (3), one gets

$$K = \frac{k\,k_1\,k_2\,V_s'\,\rho_s(1-\epsilon)}{W}\left[1 - \frac{\rho_s(1-\epsilon)}{\rho_{bs}}\right] \quad (4)$$

In this equation V_s', W, ρ_s, and ρ_{bs} are either measurable or directly calculable. ϵ is obtained through existing correlations that extend the Carman-Kozeny equation for pressure drop in a fixed granular bed into the fluidized region (*2*). Thus in the turbulent region $N_{Re'} > 30$:

$$G = \left(\frac{g_c\,\rho_F\,\phi_s}{35.4\,\mu_F^{0.44}}\right)^{0.641} \rho_s^{0.641}\,D_p^{0.923}\,\frac{\epsilon^{1.923}}{(1-\epsilon)^{0.282}} \quad (5)$$

In the laminar region $N_{Re'} < 30$:

$$G = \left(\frac{g_c\,\rho_F\,\phi_s^2}{116\,\mu_F^{0.78}}\right)^{0.082} \rho_s^{0.82}\,D_p^{1.46}\,\frac{\epsilon^{2.46}}{(1-\epsilon)^{0.416}} \quad (6)$$

When one refers to Equation (4), it is clear that a number of variables can be separated from K so that the group $k\,k_1\,k_2 \equiv K'$ instead of K is correlated with the variables to be studied.

With regard to the attrition aspect of the over-all growth mechanism the surface area of a particle is again of prime importance. When one assumes the attrition rate to be proportional to the surface area available for grinding and crushing

$$\frac{dm}{d\theta_F} = -CD^2 \quad (7)$$

where the negative sign indicates a decrease in mass. Attrition can be studied independently of normal growth by conducting runs in which no solid is deposited on the fluidized particles. Attempts have been made (*1, 8, 13*) to correlate attrition results by means of the theory of comminution. However, as pointed out by Rosin (*15*), only about 1% of the total energy consumption in pulverizers is used for crushing particles to create new surfaces. It becomes necessary then to empirically correlate the attrition coefficient C with the variables studied.

Combining Equations (2) and (7) one obtains the net growth equation

$$\frac{dm}{d\theta_F} = (K-C)D^2 \quad (8)$$

It is clear that the net growth rate may be either positive or negative depending on whether normal growth or attrition predominates. Since $m = b\rho_s D^3$, then upon differentiation and substitution in Equation (8) it follows that

$$\frac{dD}{d\theta_F} = a$$

where $a = (K-C)/3b\rho_s$. Upon integration there is obtained

$$D = D_o + a\theta_F \quad (9)$$

The over-all growth constant a is studied which involves both K and C in growth runs where feed is introduced but only C in attrition runs.

To trace particle growth with time, radioactive seed particles that are otherwise identical to those in the fluidized bed are employed. By adding a known amount of these radioactive seeds of a given activity to the starting bed of a run the growth of these seeds is followed by removing product samples at regular time intervals, analyzing them for size distribution, and determining the activity of each size fraction. The over-all growth constant can then be calculated.

It would be interesting to compare the cumulative growth of these seed particles with an equation derived by Dunlop et al. (*5*):

$$\frac{W_{SB}}{W_{SO}} = 1 + Q - e^{-\alpha'\theta_F}\left\{\sigma'^3\theta_F^3 + 3\left[\left(\frac{\sigma'}{\alpha'}\right)^2 + \sigma'^2\right]\theta_F^2 + Q(\alpha'\theta_F + 1) + 1\right\} \quad (10)$$

This equation holds before steady state is attained; at steady state the particle size distribution is predicted by weight per cent of particles in steady state mixture having a diameter of D or less

$$= 100 - \frac{100}{(1+Q)\exp\left[\left(\frac{D}{D_o}-1\right)/\left(\frac{\sigma'}{\alpha'}\right)\right]}\left[\left(\frac{D}{D_o}-1\right)^3 + 3\left(\frac{\sigma'}{\alpha'}+1\right)\left(\frac{D}{D_o}-1\right)^2 + \frac{Q}{\left(\frac{\sigma'}{\alpha'}\right)}\left(\frac{D}{D_o}-1\right) + 1 + Q\right] \quad (11)$$

EQUIPMENT, PROCEDURE, AND DATA COLLECTION

The experimental equipment consisted of a 3-in. diameter column with accessories. A schematic drawing of the complete unit is presented in Figure 1. The entire system was of stainless steel. The column was made up of two sections joined by flanges, a 14-in. fluidizing section, and a 31-in. disengagement section. The spray-nozzle assembly was installed 9 in. from the bottom of the fluidizing section, perpendicular to the axis of the column. Fluidizing gas entered through a porous sintered dis-

tributor plate bolted between the bottom flanges of the fluidizing section. The filter and blowback assembly was mounted on the top flange of the disengagement section. A vacuum sampling device was attached near the bottom of the fluidizing section.

Feed solution was introduced by either direct pumping or static air pressure in the feed tank. Direct pumping offered constant flow rate but was used only at high flow rates when surging due to pulsation between pumping cycles was not pronounced. At low feed rates the air-pressure method was used which provided smooth flow but required continual attention in flow control.

High-pressure air supplied all the requirements of the unit as shown in Figure 1. Off-gas from the unit passed through a series of water-cooled condensers before being vented. Periodic bursts of high-pressure air through timer-controlled solenoid valves returned fines accumulated on the two 3-in. porous bayonet filters to the column.

The two-fluid pneumatic spray nozzle was designed by J. J. Barghusen and D. J. Raue of ANL. The feed solution was externally atomized after being discharged from the liquid needle that protruded into the column to prevent lump formation around the nozzle. Cooling coils were soldered to the nozzle housing to eliminate prevaporization of the feed inside the nozzle.

The heating of the fluidizing section was supplied by five 1,000-w. tubular heaters wrapped around the outside of the column. A temperature controller provided on-off control as indicated by a bed thermocouple. An 800-w. band heater furnished heat to the nozzle section. Feed solution was prepared by dissolving reagent grade aluminum nitrate nonahydrate in distilled water to produce the desired concentration reported as weight per cent of the nonahydrate. The starting-bed material was obtained by first screening the calciner product aluminum oxide from ICPP into various sieve fractions and mixing them in the desired proportions. Starting beds for growth and attrition runs were composed of the following fractions:

Mesh size	Wt. %
−20+30	10
−30+40	40
−40+50	38
−50+70	10
−70+100	2

In all growth runs the − 70 + 100-mesh fraction was tracer seeds, except in runs PS-52, 53, where 2% of − 50 + 70 seeds were used.

Seeds used as tracers for detecting particle growth were obtained from radioactive calciner product aluminum oxide. The activity was due to the ruthenium − 106 isotope of 1-yr. half-life, emitting gamma radiation in its disintegration chain. This material was ground, and the − 100 + 140-mesh fraction was coated with a layer of inactive aluminum oxide in the calciner unit. Then the −, 70 + 100-mesh fraction was screened from the resulting bed and used as seeds for growth runs. This precoating procedure was necessary as the cold particles, upon direct contact

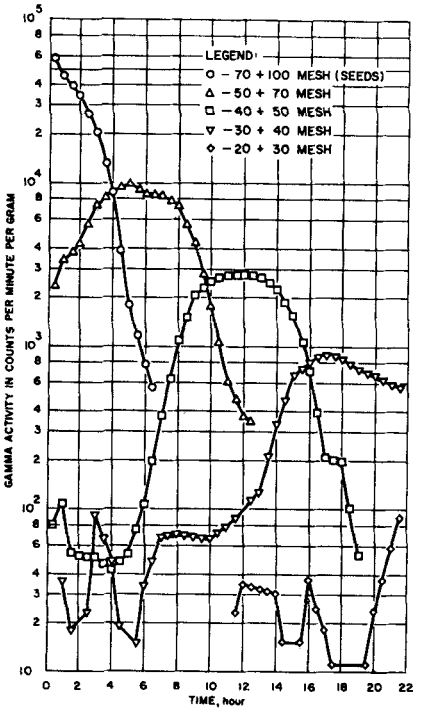

Fig. 2. Particle activity as function of time for run PS-19.

with the hot ones, became contaminated and acquired a relatively high background activity that masked the true pattern of growth, detected as the gradual acquisition of activity by successively larger sieve fractions. The precoating reduced the activity of the seeds from 10^6 to 10^5 counts/(min.)(g.) which was still quite adequate for tracing growth.

Growth runs were operated continuously for 24-hr. periods during which products were removed at regular intervals to keep the bed weight constant. Each product represented 5% or less of the bed weight so that the entire operation may be considered as one of constant bed weight. After each run each product taken during the run was separated into the following fractions: −16+20, −20+30, −30+40, −40+50, −50+70, −70+100, and −100 mesh. The weight of each fraction was recorded to provide the screen analysis of the product. Then a sample from each fraction was counted for its gamma activity.

Attrition runs were also operated for 24-hr. Every 6 hr. the entire bed was removed, screened, and then returned to the column to continue the run. Water was sprayed in as feed to simulate the conditions during growth runs.

DATA ANALYSIS

The fundamental dependent variable which indicates changes in particle size is the average diameter of the particles. Because the basic hypothesis for such changes is expressed as the proportionality between the mass rate of change of a particle and its surface area, the volume-surface mean diameter is chosen as the appropriate average diameter for this study, defined as

$$D_{vs} = \frac{\Sigma N_i D_i^3}{\Sigma N_i D_i^2} \qquad (12)$$

where N_i and D_i are taken as the arithmetic average of the openings of the two successive screens that bracket the ith sieve fraction. The summation is taken over the number of sieves used in the screen analysis. Noting that $N_i = w_i/\rho_s b D_i^3$, one reduces Equation (12) to

$$D_{vs} = \frac{\overline{W}}{\Sigma \dfrac{w_i}{D_i}} \qquad (13)$$

Growth Runs

For growth runs the change in D_{vs} with time of the seed-containing particles is followed. The number of such particles on the ith sieve is N_i in Equation (12). The seeds are of size D_o with activity A_o. From the screen analysis and the gamma count the weight w_i and the activity A_i of the ith fraction are known. Then $A_i w_i$ represents the total activity of the ith fraction. This product divided by A_o yields the weight of seeds in the ith fraction, which when divided by the weight per seed, $\rho_s b D_o^3$, yields the number of seeds in the ith fraction. If one assumes that each seed-containing particle contains one seed, then the number of seeds equals N_i. Thus when one substitutes and simplifies Equation (12) becomes

$$D_{vs} = \frac{\Sigma A_i w_i D_i^3}{\Sigma A_i w_i D_i^2} \qquad (14)$$

which is used in the calculations.

Figure 2 plots for run PS-19 the activity data vs. time. The movement of activity peaks through successive fractions clearly indicates the path of growth. It is seen that with time the activity peaks become lower as the total activity in the bed decreases with the removal of seeds in the products. Hence even a moderate background activity due to contact contamination would obscure the true activity of the larger size fractions. For this reason, in some runs where this situation existed, data for calculating D_{vs} were taken from the early part of the run when activity peaks were high and background effect was not pronounced.

When one has the set of values of D_{vs} and time, the hypothesis of a linear relationship between them as expressed in Equation (9) is tested by first calculating the best statistical straight line (*12, 17*), the least-square line, for this set of points, and then checking the linear correlation to see if it is the best correlating function. Using standard methods one makes calculations from the experimental

Table 1. Summary of Calculated Over-All Growth Constants and Experimental Conditions

Run no.	Bed weight, g.	Bed temp., °C.	Fluid.* air vel., ft./sec.	Atom.† air vel., CFM	Feed conc., wt. %	Feed rate, ml./min.	Solids** rate, g./hr.	Atom. air rate / feed rate	Over-all growth const., a, 10^4 in./hr.	K', in. lb. / hr. cu. ft.
PS-14	900	400	1.00	0.635	50	15.9	600	1,130	6.890	191.7
PS-19	900	300	1.05	0.647	50	15.9	600	1,150	6.885	191.5
PS-20	900	400	0.92	0.588	50	15.9	600	1,048	7.055	196.2
PS-26	900	300	1.00	0.554	50	15.9	600	986	7.248	202.0
PS-45	900	400	1.88	0.526	50	15.9	600	937	6.725	187.1
PS-46	900	300	1.26	0.339	50	21.2	800	453	14.24	396.0
PS-49	1,050	300	1.26	0.336	50	10.2	385	932	3.382	110.0
PS-50	1,050	300	1.40	0.321	50	10.2	385	890	3.000	97.5
PS-52	1,000	300	1.28	0.336	33	16.0	368	595	3.782	116.9
PS-53	1,000	400	1.38	0.339	33	16.1	370	596	3.703	114.3
PS-57	1,100	400	1.86	0.321	50	10.2	385	890	2.760	94.0
PS-58	1,100	400	1.88	0.749	50	10.0	378	2,120	1.850	63.0
PS-59	1,100	400	1.86	0.653	50	9.6	364	1,930	1.727	58.8
PS-60††	1,100	400	1.57	0.329	50	9.6	364	970	2.795	95.2
PS-61***	1,100	400	1.52	0.329	50	9.6	364	970	2.758	94.0

* Fluidizing air velocity at column temperature and pressure
† Atomizing air rate at column pressure but room temperature.
** Solids rate as grams per hour of aluminum nitrate nonahydrate.
†† Surface tension of feed reduced by 1.63 by adding 0.012 wt. % of Tween 20.
*** Viscosity of feed increased by 5.15 by adding 0.125 wt. % of Natrosol.

data of D_{vs} and θ_F for the least-square constants, λ and ν, in

$$D_{vs} = \lambda + \nu\,\theta_F \qquad (15)$$

The goodness of the correlation is measured by a correlation coefficient r, which is unity for perfect correlation and zero for no correlation. Statistical tables are available that list the probability of getting a value of r larger than the experimental one when there is no correlation between the variables.

Another test for significance of correlation is the F-test (*12*). A test of the validity of the linear behavior of the data may be obtained by calculating a statistic F and then consulting standard statistical tables for the probability levels for finding values of F greater than the calculated ones.

In every run the correlation coefficient is greater than 0.95, and the F-test shows correlation significance greater than 0.95, strongly confirming the original hypothesis of the proportionality between the growth rate and the surface area of a particle. Similar result was reported (*5*) in a fluidized coker. Thus the least-square constant ν is the best estimate of the over-all growth constant a. A summary of the over-all growth constants calculated from least-square method for all the runs at their respective experimental conditions is presented in Table 1.

When the F-test proves the correlation significant, the best estimate of the precision of ν can be calculated. The average precision for runs reported is ± 6%.

Good reproducibility of the data was found through two runs, PS-59 duplicating PS-58, and PS-26 duplicating PS-19. A 7% difference between the values of ν for PS-58 and PS-59 is accounted for by the slightly lower feed rate in PS-59, while a higher value of atomizing air to feed ratio in PS-19 accounts for the 5% difference in ν between PS-19 and PS-26.

Attrition Runs

A series of four 24-hr. runs was made to check the effect of operating variables on attrition and the relative magnitude of attrition with respect to normal growth. The operating conditions for these runs are summarized in Table 2. To calculate D_{vs} Equation (13) is applied directly to the data. The effect of sampling location was tested by taking samples from both the top and the bottom of the bed in some runs.

Next, a statistical test, the Student-t, is applied to the results to test for significance of the effect of the following factors on attrition: column temperature, fluidizing velocity, sampling location, and atomizing air to feed ratio. From standard tables the calculated value of the statistic t is compared for significance against the tabulated one at 95% confidence. The effect of all the above factors on attrition are found to be nonsignificant. Then, since these factors are the most important ones from physical considerations, the attrition effect is nonsignificant, at least relative to normal growth.

CORRELATION OF DATA

Since attrition effect is found to be a nonsignificant one, then the over-all growth constant a is solely determined by the normal growth coefficient K; that is $K = 3b\rho_s a$. When one combines this with Equation (4), K' is correlated with the variables studied. Thus

$$K' = \frac{3abW}{V_s'(1-\epsilon)}\left[1 - \frac{\rho_s(1-\epsilon)}{\rho_{bs}}\right]^{-1} \equiv \Psi a \qquad (16)$$

In the above equation V_s' is calculated from the geometry of the column and the characteristics of the spray nozzle (*9*):

$$V_s' = \frac{\pi}{12} D_c^2 \tan^2\psi \cos\psi\,(2 + \sin^2\psi) \qquad (17)$$

Table 2. Summary of Operating Conditions for Attrition Runs

Run no.	Column temp., °C.	Fluidizing velocity, ft./sec.	Water feed rate, ml./min.	Atom. air rate / feed rate (volume ratio)
AT-1	300	1.3	16	660
AT-1′	400	1.3	16	660
AT-2	300	1.3	10.4	1,370
AT-4	300	1.8	10.4	1,370

Particle properties are then determined from direct measurements, and ϵ is calculated with either Equation (5) or (6).

Density measurements by the xylene displacement method for products at the beginning, middle, and end of runs at both 300° and 400°C. showed only small variation, and an average of 1.77 g./cc. was obtained. The volume shape factor b was determined from a weighed sample M of a given sieve fraction by counting the number of particles N in it: $b = M/(\rho_s N D^3)$. Products of different sizes at the beginning and end of a run yielded an average value of $b = 0.542$. For a spherical particle $b = \pi/6 = 0.524$. Thus the particles were quite spherical confirming a similar conclusion from visual observations, the approach to sphericity being 0.96. The surface shape factor ϕ_s, defined as the ratio of the surface area of a spherical particle having the same volume as the given particle to the surface of that particle, could not in general be determined accurately. As the particles involved were almost spherical, a value of 0.96 was assigned to ϕ_s. The bulk density ρ_{bs} and the average size of particles in the bed D_p were calculated directly from the weight of a given volume of particles and Equation (13), respectively, at the beginning and end of each run and an average value taken.

To determine the bed voidage ϵ the fluidized bed was assumed to be in the laminar region, that is where $N_{Re'} < 30$. Then Equation (6) was used to obtain ϵ, after which $N_{Re'}$ was calculated with this value of ϵ to see if it was below 30. In this manner values of ϵ and $N_{Re'}$ for each run were obtained, and all the values of $N_{Re'}$ were found to be below 30 as originally assumed.

Now in Equation (16) for each run Ψ would be calculated, whence K'. However the group $\rho_s(1-\epsilon)/\rho_{bs}$ was close to unity in a number of runs so that upon taking difference between it and unity any small uncertainty in the group would be magnified greatly in the difference. Consequently as the value of ρ_{bs} for these runs was quite constant and those for ϵ reasonably so, average value of each was used for all the runs. Then $\Psi = 1.40 \times 10^5 W$, and the last column of Table 1 presents the values of K' thus calculated.

To relate K' with the variables studied the proposed correlation is

$$K' = \phi \left(\frac{F}{W}\right)^{\alpha} B^{\beta} V^{\gamma} T^{\delta} \mu^{\omega} \sigma^{\tau} \quad (18)$$

The inclusion of F/W instead of F is apparent because it is the amount of feed available to each particle that

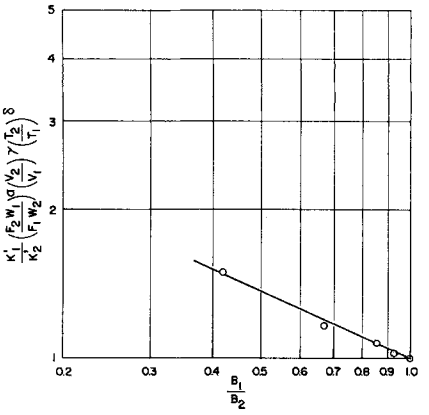

Fig. 3. Determination of the exponent β in the correlation equation for K'.

determines the extent of growth. The form is dictated from physical considerations by the presence of only primary actions of the variables on K' and the absence of interactions between them. It is known that the combined effect of a group of variables not mutually dependent is best described by a product form. The various exponents in Equation (18) are evaluated one at a time. A number of runs are selected in which all the variables but one are held constant. The exponent of that variable is obtained by plotting ratios of K' between pairs of runs vs. ratios of that variable on log-log paper. If a straight line through the point (1, 1) should result, then the slope of this line is the exponent of that variable. The goodness of the fit of Equation (18) to the data is measured first by the degree of linearity in plotting the above-mentioned ratios, and secondly by the constancy of ϕ calculated from all the runs. In this manner the various exponents are determined. An example of such plots

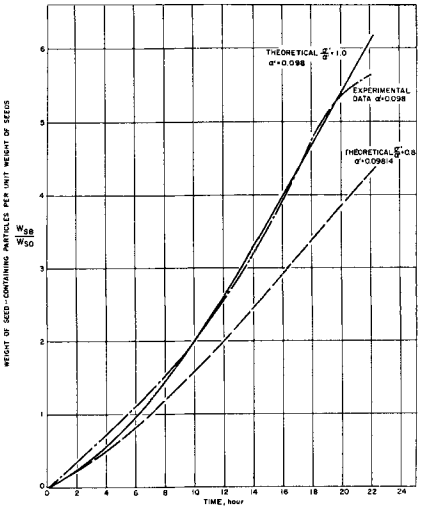

Fig. 4. Comparison of calculated and predicted cumulative growth curves for seed particles for run PS-19.

is shown in Figure 3, whereby the exponent β is determined. Then ϕ is calculated from each run and found to be quite constant at 3×10^4. Thus the final form of the correlation equation is

$$K' = 3 \times 10^4 \left(\frac{F}{W}\right) B^{-0.5} V^{-0.1} \mu^{0.08} \sigma^{-0.3} \quad (19)$$

and

$$K = \frac{1 \times 10^4 \left(\frac{F}{W}\right) B^{-0.5} V^{-0.1} \mu^{0.08} \sigma^{-0.3} V_s'(1-\epsilon)}{bW \left[1 - \frac{\rho_s(1-\epsilon)}{\rho_{bs}}\right]} \quad (20)$$

Equation (20) correlates the data to an average absolute deviation of 4% and an arithmetic average of 0.07%.

COMPARISON WITH OTHER WORK

It would be of interest to compare the cumulative growth of seed-containing particles as predicted by Equation (10) with the present data. Agreement is expected, as Equation (10) is derived assuming only the validity of a linear increase of particle diameter with time and a time-decay type of equation for the removal of seed particles. To check this, data from run PS-19 are used to calculate W_{SB}/W_{SO} as a function of time and the results compared with the curve predicted from Equation (10).

For a run in which initially seeds of weight W_{SO} and diameter D_o having activity A_o are added to the system the weight of seeds W_{Si} present in the ith sieve fraction of the jth product is given by $(A_i w_i / A_o)_j$. The weight of particles containing these seeds is $W_{SB_{ij}} = \left[\frac{A_i w_i}{A_o}\left(\frac{D_i}{D_o}\right)^3\right]_j$. The weight of such particles in the jth product per unit weight of seeds is $\left(\frac{W_{SB}}{W_{SO}}\right)_j = \left[\frac{1}{A_o W_{SO}} \sum_i A_i w_i \left(\frac{D_i}{D_o}\right)^3\right]_j$. This quantity is calculated for each product withdrawn at successive time intervals. Then the cumulative weight of such particles from product one through k is given by $\sum_{j=1}^{k} \left(\frac{W_{SB}}{W_{SO}}\right)_j$.

When one follows this procedure, data from PS-19 are analyzed and results plotted as the experimental curve in Figure 4. Then using the value of the over-all growth constant a previously calculated and known values of α' and D_o one can plot the theoretical curve with $\sigma'/\alpha' = 1.0$ for PS-19. To show

the sensitivity of the theoretical curve another curve with $\sigma'/\alpha' = 0.8$ is also shown. Figure 4 indicates good agreement between the experimental and theoretical curves. Since Equation (10) holds satisfactorily prior to steady state, Equation (11) directly derived from it should hold; that is to say the steady state distribution of particles can be predicted from Equation (11).

CONCLUSION

It has been demonstrated in this investigation that radioactive tracer can be employed to successfully follow the mechanism of particle growth in a fluidized calciner. The hypothesis that the mass rate of growth of a particle is proportional to its surface area is substantiated.

Of the two major factors contributing to over-all growth studied in this work it has been found that attrition exerts a nonsignificant effect compared with normal growth, and hence over-all growth is determined by normal growth. The influence of operating variables and physical properties of the feed system has been investigated with the result that the feed-to-bed weight ratio and the atomizing air-to-feed ratio are found to be of prime importance. The normal growth coefficient has been correlated with the variables studied.

For steady state operation seeds must be introduced into the calciner to balance the normal growth. Direct addition of seeds to the calciner is one possibility. Other methods of creating seeds such as jet or target grinding have been reported (5). When one has such data to counteract normal growth, conditions for no net particle growth can then be derived and steady state operation achieved.

ACKNOWLEDGMENT

The experimental investigation was sponsored by and conducted at Argonne National Laboratory under an Atomic Energy Commission contract.

The appointment to B. S. Lee to carry out the research on this work and the generous support and cooperation of all the friends in the Argonne Chemical Engineering Division are hereby gratefully acknowledged.

NOTATION

A_c = column cross-sectional area, sq. ft.
A = activity of particles, counts/(min.)(g.)
a = over-all growth constant, in./hr.
B = volume ratio of atomizing air rate to feed rate, dimensionless
b = volume shape factor, dimensionless
C = attrition coefficient, lb./(hr.)(ft.)^2
D = diameter of a particle, ft.
D_c = diameter of column, in.
D_i = average particle size on ith sieve, in.
D_o = initial diameter, ft.
D_p = average diameter of particles in a fluidized bed, ft.
D_{vs} = volume-surface mean diameter of particles, in.
F = solids feed rate, g./hr.
g_c = gravitational constant, ft./hr.^{2}
G = mass velocity of fluidizing air, lb./(hr.)(ft.)^2
k, k_1, k_2 = constants defined in deriving Equation (3)
K = normal growth coefficient, lb./(hr.)(ft.)^2
K' = constant equal to $k\,k_1\,k_2$
L_F = fluidized bed height, ft.
L_s = static bed height, ft.
L_o = fictitious bed height with no voids, ft.
m = mass of a single particle, lb.
N_i = number of particles on ith sieve
$N_{Re'}$ = modified Reynolds number $= D_p G/\mu_F(1-\epsilon)$, dimensionless
Q = constant equal to $6(\sigma'/\alpha')^3 + 6(\sigma'/\alpha')^2 + 3(\sigma'/\alpha')$, dimensionless
T = temperature, °C.
V = fluidizing linear velocity, ft./sec.
V_s' = volume of spray cone in empty column, cu. ft.
V_s = volume of spray cone, cu. ft.
V_T = volume of fluidized bed, cu. ft.
W = weight of fluidized bed, lb.
$\overline{W}$ = weight of a sample, g.
W_{SB} = weight of seed-containing particles, g.
W_{SO} = weight of seeds initially, g.
w = weight of a sieve fraction, g.

Greek Letters

$\alpha, \beta, \gamma, \delta, \omega, \tau, \phi$ = exponents and constant defined in Equation (18)
α' = ratio of weight rate of product withdrawal to the total weight of bed, 1/hr.
ϵ = bed voidage fraction, dimensionless
θ_F = residence time in fluidized bed, hr.
θ_s = residence time in spray zone, hr.
λ, ν = constants defined in Equation (15)
μ = viscosity of feed, lb./(hr.)(ft.)
μ_F = viscosity of fluidizing gas, lb./(hr.)(ft.)
ρ_F = fluidizing gas density, lb./cu. ft.
ρ_s = solids density, lb./cu. ft.
ρ_{bs} = bulk density of static bed, g./cc.
ρ_{bF} = bulk density of fluidized bed, g./cc.
σ = surface tension of feed, dynes/cm.
σ' = a/D_o
ϕ_s = surface shape factor, dimensionless
ψ = half spray angle for the nozzle, deg.

LITERATURE CITED

1. Bond, F. C., *Trans. Am. Inst. Mining Met. Petrol. Engrs.*, **193**, 484 (May, 1952).
2. Chu, J. C., James Kalil, and W. A. Wetteroth, *Chem. Eng. Progr.*, **49**, 141 (1953).
3. Dawerval, F. B., et. al., *Atomic Energy Commission Research and Development Reports*, MCW-1421 (1958); MCW-1426 (1959); MCW-1429 (1959); MCW-1431 (1959); MCW-1433 (1959); MCW-1442 (1960).
4. Duffie, J. A., and W. R. Marshall, Jr., *Chem. Eng. Progr.*, **49**, 417, 480 (1953).
5. Dunlop, D. D., L. I. Griffin, Jr., and J. F. Moser, Jr., *ibid.*, **54**, 39 (1958).
6. Grimmett, E. S., *Atomic Energy Commission Research and Development Reports*, IDO-14416 (1957); IDO-14471 (1959).
7. Jonke, A. A., E. J. Petkus, J. W. Loeding, and Stephen Lawroski, *Nuc. Sci. Eng.*, **2**, 303 (1957).
8. Kick, Friedrich, "Das Gesetz der proportionalen Widerstande und seine Anwendung," Arthur Felix, Leipzig, Germany (1855).
9. Lee, B. S., D.Ch.E. dissertation, Polytech. Inst. Brooklyn, New York (June, 1960).
10. Loeding, J. W., A. A. Jonke, et al., *Proc. Second United Nations Conf. on the Peaceful Uses of Atomic Energy, Geneva*, **18**, 56 (1958).
11. Meyer, F. W., *Chem. Eng. Progr.*, **51**, 528 (1955).
12. Mickley, H. S., T. K. Sherwood, and C. E. Reed, "Applied Mathematics in Chemical Engineering," McGraw-Hill, New York (1957).
13. Rittinger, von, P. R., "Lehrbuch der Aufbereitungskunde," Ernst and Korn, Berlin, Germany (1867).
14. Rodger, W. A., *Argonne National Laboratory*, private communication (April, 1960).
15. Rosin, P. O., *Trans. Inst. Chem. Engrs. (London)*, **15**, 167 (1937).
16. Sanders, E. F., et. al., *Atomic Energy Commission Research and Development Reports*, MCW-1409 (1957); MCW-1411 (1958).
17. Volk, W., "Applied Statistics for Engineers," McGraw-Hill, New York (1958).
18. Wolman, Abel, and A. E. Gorman, *Chem. Eng. Progr.*, **51**, 470 (1955).

Manuscript received December 29, 1960; revision received May 23, 1961; paper accepted May 26, 1961.